

Quantum State Engineering with Continuous-Variable Post-Selection

Andrew M. Lance,¹ Hyunseok Jeong,² Nicolai B. Grosse,¹ Thomas Symul,¹ Timothy C. Ralph,² and Ping Koy Lam¹

¹Quantum Optics Group, Department of Physics, Faculty of Science, Australian National University, ACT 0200, Australia

²Department of Physics, University of Queensland, St Lucia, Queensland 4072, Australia

(Dated: February 1, 2008)

We present a scheme to conditionally engineer an optical quantum system via continuous-variable measurements. This scheme yields high-fidelity squeezed single photon and superposition of coherent states, from input single and two photon Fock states respectively. The input Fock state is interacted with an ancilla squeezed vacuum state using a beam splitter. We transform the quantum system by post-selecting on the continuous-observable measurement outcome of the ancilla state. We experimentally demonstrate the principles of this scheme using coherent states and measure experimental fidelities that are only achievable using quantum resources.

Introduction - The transformation or engineering of quantum states via measurement induced conditional evolution is an important technique for discrete variable systems, particularly in the field of quantum information [1]. Typically, the quantum system of interest is interacted with a prepared ancilla state, which is then measured in a particular basis. The system state is retained, or discarded, depending on the measurement outcome, resulting in the controlled conditional evolution of the quantum system. It is a necessary condition for inducing a non-trivial conditional evolution that the interaction of the ancilla and system produces entanglement between them.

In optical systems, highly non-linear evolutions, which are difficult to induce directly, can be induced conditionally on systems by post-selecting on particular photon counting outcomes [2]. In principle, a near deterministic, universal set of unitary transformations can be induced on optical qubits in this way [3]. Importantly, it was shown that arbitrary optical states can be engineered conditionally, based on discrete single photon measurements [4].

Recently, there has been increased interest in conditional evolution based on continuous-variable measurements [5, 6, 7]. In these schemes a quantum system is interacted with a prepared ancilla, which is measured via a *continuous* observable, e.g. the amplitude or phase quadratures of the electromagnetic field. This has been experimentally demonstrated for a system using a beamsplitter as the interaction and a vacuum state as the ancilla, with conditioning based on homodyne detection [6]. A similar system using conditioning of adaptive phase measurements has also been studied [7].

In this letter, we investigate a continuous-variable conditioning scheme based on a beam splitter interaction, homodyne detection and an ancilla squeezed vacuum state. We theoretically show that for input one and two photon Fock states, this scheme yields high fidelity squeezed single photon Fock states and superposition of coherent states (SCS) respectively, which are highly non-classical and interesting quantum states that have potentially useful applications in quantum information processing [8]. We experimentally demonstrate the principles of this scheme using input coherent states, and measure experimental fidelities that are only achievable using quantum resources.

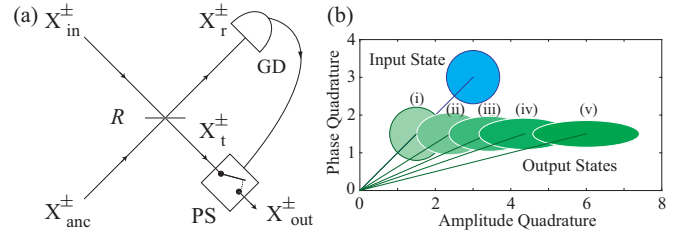


FIG. 1: (Color online) (a) Schematic of the post-selection protocol. \hat{X}_{in}^{\pm} : amplitude (+) and phase (-) quadratures of the input state; (anc) ancilla state; (r) reflected; (t) transmitted; and (out) post-selected output state. R : beam splitter reflectivity; GD: gate detector; PS: post-selection protocol. (b) Standard deviation contours of the Wigner functions of an input coherent state (blue) and post-selected output states (green) for $R = 0.75$ and varying ancilla state squeezing of (i) $s = 0$, (ii) $s = 0.35$, (iii) $s = 0.69$, (iv) $s = 1.03$ and (v) ideal squeezing.

Theory - The squeezed vacuum ancilla state used in our scheme is represented as $\hat{S}(s)|0\rangle$ with the squeezing operator $\hat{S}(s) = \exp[-(s/2)(\hat{a}^2 - \hat{a}^{\dagger 2})]$, where s is the squeezing parameter and \hat{a} is the annihilation operator. The Wigner function of the squeezed vacuum is $W_{sqz}(\alpha; s) = 2 \exp[-2(\alpha^+)^2 e^{-2s} - 2(\alpha^-)^2 e^{2s}]/\pi$, where $\alpha = \alpha^+ + i\alpha^-$ with real quadrature variables α^+ and α^- . The first step of our transformation protocol is to interfere the input field with the ancilla state on a beam splitter as shown in Fig. 1 (a). The beam splitter operator \hat{B} acting on modes a and b is represented as $\hat{B}(\theta) = \exp\{(\theta/2)(\hat{a}^{\dagger}\hat{b} - \hat{b}^{\dagger}\hat{a})\}$, where the reflectivity is defined as $R = \sin^2(\theta/2)$ and $T = 1 - R$. A homodyne measurement is performed on the amplitude quadrature on the reflected field mode, with the measurement result denoted as X_r^+ . The transmitted state is post-selected for $|X_r^+| < x_0$, where the post-selection threshold x_0 is determined by the required fidelity between the output state and the ideal target state.

We first consider a single-photon state input, $|1\rangle$, and a squeezed single photon, $\hat{S}(s')|1\rangle$, as the target state. The Wigner function of the single photon state is $W_{in}^{(1)}(\alpha) = 2 \exp[-2|\alpha|^2](4|\alpha|^2 - 1)/\pi$. After interference via the beam

splitter, the resulting two-mode state becomes $W(\alpha, \beta) = W_{\text{in}}^{(1)}(\sqrt{T}\alpha + \sqrt{R}\beta)W_{\text{anc}}(-\sqrt{R}\alpha + \sqrt{T}\beta)$, where $W_{\text{anc}} = W_{\text{sqz}}(\alpha; s)$ and $\beta = \beta^+ + i\beta^-$. The transmitted state after the homodyne detection of the reflected state is $W_{\text{out}}(\alpha; X_r^+) = P_1(X_r^+)^{-1} \int_{-\infty}^{\infty} d\beta^- W(\alpha, \beta^+ = X_r^+, \beta^-)$, where the normalization parameter is $P_1(X_r^+) = \int_{-\infty}^{\infty} d^2\alpha d\beta^- W(\alpha, \beta^+ = X_r^+, \beta^-)$. If the measurement result is $X_r^+ = 0$, the Wigner function of the output state becomes

$$W_{\text{out}}(\alpha) = \frac{2}{\pi} e^{-2[e^{-2s'}(\alpha^+)^2 + e^{2s'}(\alpha^-)^2]} \times (4e^{-2s'}(\alpha^+)^2 + 4e^{2s'}(\alpha^-)^2 - 1), \quad (1)$$

where $s' = -\ln[(T + e^{-2s}R)^2]/4$. One can immediately notice that the output state in Eq. (1) is *exactly* the Wigner function of a squeezed single photon, $\hat{S}(s')|1\rangle$. We note that the output squeezing s' can be arbitrarily close to the squeezing of the ancilla state s by making R close to zero. For the nonzero post-selection threshold criteria $|X_r^+| < x_0$, the corresponding success probability is given by $P_s(x_0) = \int_{-x_0}^{x_0} dX_r^+ P_1(X_r^+)$.

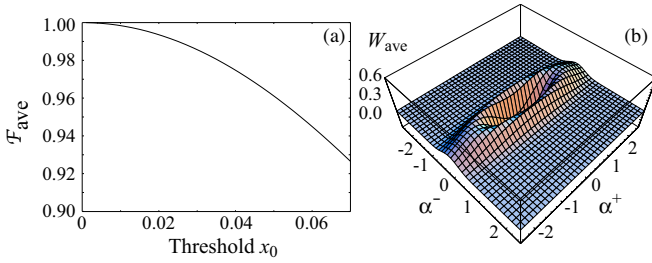


FIG. 2: (Color online) (a) The average fidelity \mathcal{F}_{ave} between the post-selected output state of an input single photon state $|1\rangle$, and the squeezed single photon state $\hat{S}(s')|1\rangle$, for varying threshold x_0 . The beam splitter reflectivity is $R = 0.98$, ancilla state squeezing is $s = 0.7$ and target state squeezing is $s' = 0.67$. (b) The average Wigner function W_{ave} of the output state for $\mathcal{F}_{\text{ave}} = 0.99$, for $x_0 = 0.025$ and $P_s = 0.003$.

We calculate the fidelity between the output state (with the measurement result X_r^+) and the ideal target state given by $\mathcal{F}_1(X_r^+) = \pi \int_{-\infty}^{\infty} d^2\alpha W_{\text{out}}(\alpha; X_r^+) W_{\text{out}}(\alpha)$. From this we can determine the average fidelity for the threshold x_0 defined as $\mathcal{F}_{\text{ave}}(x_0) = \int_{-x_0}^{x_0} dx P_1(X_r^+) \mathcal{F}_1(X_r^+) / \int_{-x_0}^{x_0} d\tilde{X}_r^+ P_1(\tilde{X}_r^+)$. We use this average fidelity measure to characterize the efficacy of our protocol for nonzero thresholds. We can likewise determine the average Wigner function $W_{\text{ave}}(\alpha; x_0)$ for the threshold x_0 .

Fig. 2 (a) shows the average fidelity \mathcal{F}_{ave} for varying post-selection threshold x_0 . This figure illustrates that high fidelity squeezed single photon states can be produced using experimentally realizable squeezing of the ancilla state and finite thresholds. The average Wigner function corresponding to an average fidelity $\mathcal{F}_{\text{ave}} = 0.99$ is shown in Fig. 2 (b). We point out that post-selection around $X_r^+ = 0$ preserves the non-

Gaussian features of the input state. Our scheme enables one to perform the squeezing of a single photon with high fidelities using any *finite* degree of squeezing of the ancilla state. We point out that this squeezed single photon state is a good approximation to an odd SCS, which has applications in quantum information processing [8]. We emphasize that this interesting result *cannot* be achieved by continuous electro-optic feed-forward methods [10] with finite ancilla state squeezing.

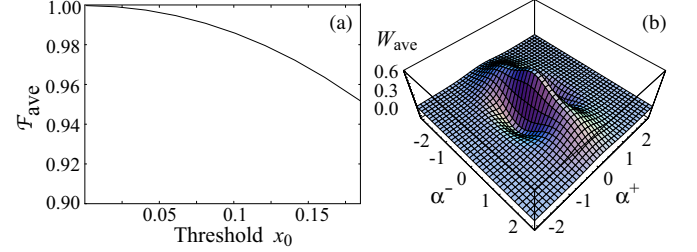


FIG. 3: (Color online) (a) The average fidelity \mathcal{F}_{ave} between the output state of the input two photon state, $|2\rangle$, and the ideal superposition of coherent states (SCS), for varying threshold x_0 . The beam splitter reflectivity is $R = 1/2$, the ancilla state squeezing is $s = -0.37$, and the amplitude of the SCS is $\gamma = 1.1i$. (b) The average Wigner function W_{ave} of the output state for $\mathcal{F}_{\text{ave}} = 0.99$, for $x_0 = 0.084$ and $P_s = 0.052$.

Another example of our post-selection protocol is for the case of input two-photon Fock states, $|2\rangle$. In this case, our target state is an even SCS, $|\gamma\rangle + |-\gamma\rangle$ (unnormalized), where $|\gamma\rangle$ is a coherent state of amplitude $\gamma = \gamma^+ + i\gamma^-$. The Wigner representation of the SCS is

$$W_{\text{scs}}(\alpha) = N_1 \left\{ e^{-2|\alpha - \gamma|^2} + e^{-2|\alpha + \gamma|^2} + e^{-2|\gamma|^2} (e^{-2(\alpha + \gamma)^*(\alpha - \gamma)} + e^{-2(\alpha + \gamma)(\alpha - \gamma)^*}) \right\}, \quad (2)$$

where $N_1 = \{\pi(1 + e^{-2|\gamma|^2})\}^{-1}$. For an input two photon Fock state, the fidelity between the post-selected output state (with the measurement result X_r^+) and the ideal SCS target state is $\mathcal{F}_2(X_r^+) = \pi \int_{-\infty}^{\infty} d^2\alpha W_{\text{out}}(\alpha; X_r^+) W_{\text{scs}}(\alpha)$. From this expression, the average fidelity \mathcal{F}_{ave} and average Wigner function W_{ave} for a post-selection threshold x_0 can be calculated. Fig. 3 shows the average fidelity of the output state for varying threshold, which illustrates that high fidelity SCS can be obtained with experimentally realizable ancilla state squeezing and finite thresholds. The average Wigner function corresponding to an average fidelity of $\mathcal{F}_{\text{ave}} = 0.99$ is shown in Fig. 3 (b). Once such SCSs are obtained, they can be conditionally amplified for SCSs of larger amplitudes using only linear optics schemes [9].

We now consider the case of a Gaussian state, i.e., an *unknown* coherent state, $|\gamma\rangle$, as the input. The post-selection scheme for $X_r^+ = 0$ transforms the coherent state as

$$D(\gamma)|0\rangle \longrightarrow D(\sqrt{T}[e^{2s'}\gamma^+ + i\gamma^-])S(s')|0\rangle, \quad (3)$$

where $D(\gamma) = \exp[\gamma\hat{a}^\dagger - \gamma^*\hat{a}]$ is the displacement operator. Figure 1 (b) illustrates that the squeezing and the displacement transformation of the post-selected output state

in Eq. (3) is dependent on the ancilla state squeezing, and that the output state is a minimum uncertainty state independent of the ancilla state squeezing. In the limit of ideal ancilla state squeezing, the post-selection scheme works as an ideal single-mode squeezer for arbitrary input coherent states $D(\gamma)|0\rangle \rightarrow S(s')D(\gamma)|0\rangle$. In this case, the output squeezing is $s' \rightarrow -\ln[T]/2$. We note that for input coherent states this scheme provides an alternative method of squeezing to electro-optic protocols presented in [10].

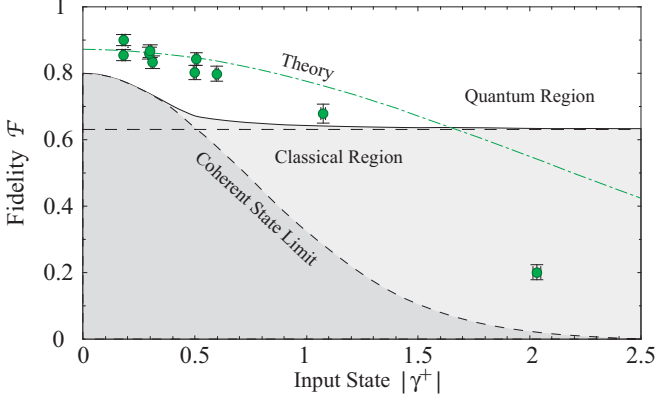


FIG. 4: (Color online) Experimental fidelity for varying amplitudes $|\gamma^+|$ of the input coherent state, for $R = 0.75$ and $x_0 = 0.01$. Dark grey region: classical fidelity limit for an ancilla vacuum state; Light grey region: classical fidelity limit. Dot-dashed line: calculated theoretical prediction of experiment, with experimental losses and inefficiencies.

Experiment - We experimentally demonstrated the principle of the post-selection protocol using input displaced coherent states for a realizable ancilla state squeezing. For the experiment, the quantum states we considered reside at the sideband frequency (ω) of the electromagnetic field. We denote the quadratures of these quantum states as $\hat{X}^\pm = \langle \hat{X}^\pm \rangle + \delta \hat{X}^\pm$, where $\langle \hat{X}^\pm \rangle$ are the mean quadrature displacements, and where the quadrature variances are expressed by $V^\pm = \langle (\delta \hat{X}^\pm)^2 \rangle$.

Fig. 1 shows the experimental setup. We used a hemilithic MgO:LiNbO₃ below-threshold optical parametric amplifier, to produce an amplitude squeezed field at 1064 nm with squeezing of $s = 0.52 \pm 0.03$, corresponding to a quadrature variance of $V_{\text{anc}}^+ = -4.5 \pm 0.2$ dB with respect to the quantum noise limit. More detail of this experimental production of squeezing is given in [11]. The displaced coherent states were produced at the sideband frequency of 6.81 MHz of a laser field at 1064 nm, using standard electro-optic modulation techniques [11]. The post-selection protocol goes as follows: the amplitude squeezed ancilla field \hat{X}_{anc}^\pm was converted to a phase squeezed field by interfering it with the input coherent state \hat{X}_{in}^\pm with a much larger coherent amplitude on the beam splitter with a relative optical phase shift of $\pi/2$. This optical interference yielded two output states that were phase squeezed. The optical fringe visibility between the two

fields was $\eta_{\text{vis}} = 0.96 \pm 0.01$.

We directly detected the amplitude quadrature of the reflected state \hat{X}_r^+ using a gate-detector, which had a quantum efficiency of $\eta_{\text{det}} = 0.92$ and an electronic noise of 6.5 dB below the quantum noise limit. The post-selection could, in principle, be achieved using an all optical setup, but here we post-selected *a posteriori* the quadrature measurements of the transmitted state, \hat{X}_t^\pm , which were measured using a balanced homodyne detector. The total homodyne detector efficiency was $\eta_{\text{hom}} = 0.89$, with the electronic noise of each detector 8.5 dB below the quantum noise limit. To characterize the protocol, we also measured the quadratures of the input coherent state, \hat{X}_{in}^\pm , using the same homodyne detector. To ensure accurate results, the total homodyne detector inefficiency was inferred out of all quadrature measurements [11].

The electronic photocurrents of the detected quantum states (at a sideband frequency of 6.81 MHz) from the gate and homodyne detectors were electronically filtered, amplified and demodulated down to 25 kHz using an electronic local oscillator at 6.785 MHz. The resulting photocurrents were digitally recorded using a NI PXI 5112 data acquisition system at a sample rate of 100 kS/s. We used computational methods to filter, demodulate and down-sample the data, so that it could be directly analyzed in the temporal domain. From this data, we post-selected the quadrature measurements of the transmitted state, \hat{X}_t^\pm , which satisfied the threshold criteria $|X_r^+| < x_0$. This post-selection threshold was independent of the input state and was experimentally optimized depending on the beam splitter reflectivity.

We characterized the efficacy of our protocol as an ideal single mode squeezer, by determining the fidelity of the post-selected output state with a target state that is an ideal squeezed operation of the input state [Eq. (3)]. The Wigner function of this ideal squeezed input state is given by $W_{\text{out}}(\gamma; s')$, where $s \rightarrow \infty$ and $s' \rightarrow -\ln[T]/2$. In this case, the fidelity is given by $\mathcal{F}(X_r^+) = \pi \int_{-\infty}^{\infty} d^2\gamma W_{\text{expt}}(\gamma; X_r^+) W_{\text{out}}(\gamma; s')$, where $W_{\text{expt}}(\gamma; X_r^+)$ is the Wigner function of the post-selected output state. From this expression the average fidelity \mathcal{F}_{ave} for a post-selection threshold x_0 can be calculated. This corresponds to unity fidelity $\mathcal{F}_{\text{ave}} = 1$ in the limit of ideal ancilla state squeezing and $X_r^+ = 0$. In the experiment, the input state was a slightly mixed state due to inherent low-frequency classical noise on the laser beam, with quadrature variances of $V_{\text{in}}^+ = 1.13 \pm 0.02$ and $V_{\text{in}}^- = 1.05 \pm 0.02$, with respect to the quantum noise limit. Hence, we calculated the fidelity of the post-selected output state with an ideal squeezed transform of the experimental input state. Fig. 4 shows the classical fidelity limit $\mathcal{F}_{\text{clas}}$, which signifies the highest fidelity achievable when the interaction of the ancilla and input coherent state yields no entanglement. Exceeding this classical fidelity limit can only be achieved using quantum resources.

Fig. 4 shows the experimental fidelity for varying input states $|\gamma^+| \equiv |\langle \hat{X}_{\text{in}}^+ \rangle|$. For a beam splitter reflectivity of $R = 0.75$, we achieved a best fidelity of $\mathcal{F}_{\text{ave}} = 0.90 \pm 0.02$ for an input state $|\gamma^+| = 0.18 \pm 0.01$, which exceeds the

maximum classical fidelity of $\mathcal{F}_{\text{clas}} = 4/5 = 0.8$. This post-selected output state had quadrature variances of $V_{\text{out}}^+ = 4.70 \pm 0.11$ and $V_{\text{out}}^- = 0.51 \pm 0.01$. The mean quadrature displacement gains, $g^\pm = \langle \hat{X}_{\text{out}}^\pm \rangle / \langle \hat{X}_{\text{in}}^\pm \rangle$, were measured to be $g^+ = 0.71 \pm 0.16$ and $g^- = 0.50 \pm 0.06$. This is compared with the ideal case of perfect ancilla state squeezing, where the ideal theoretical gains are $g_{\text{ideal}}^+ = 2$ and $g_{\text{ideal}}^- = 1/2$. The phase gain was controlled by the beam splitter transmittivity, whilst the amplitude gain was less the ideal case due to finite ancilla state squeezing, finite post-selection threshold and experimental losses.

The quantum nature of the post-selection protocol is demonstrated by the experimental fidelity results that exceed the classical fidelity limit in Fig. 4. For large input states $|\gamma^+|$, the experimental fidelity was less than the theoretical prediction due to electronic detector noise and the finite resolution of the data acquisition system, resulting in a smaller post-selected output state $|\gamma^+|$ and a corresponding decrease in the experimental fidelity. Fig. 5 (a) illustrates how the experimental fidelity of a post-selected state transitions to the quantum fidelity region by decreasing the post-selection threshold (and corresponding probability of success).

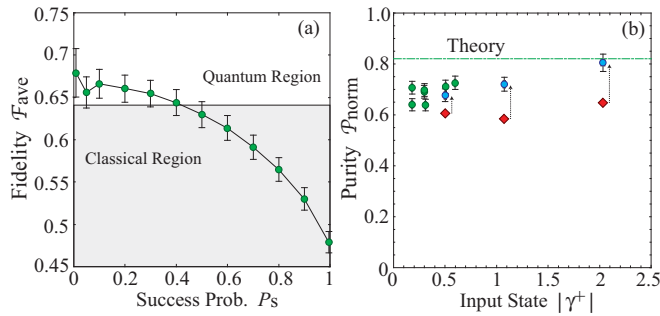


FIG. 5: (Color online) (a) Experimental fidelity (\mathcal{F}_{ave}) for varying post-selection success probability, for an amplitude $|\gamma^+| = 1.07$ of the input state and $R = 0.75$. (b) Experimental purity ($\mathcal{P}_{\text{norm}}$) for varying input state $|\gamma^+|$, for $x_0 = 0.01$. Dash arrows show purity prior to (diamonds) and after (circles) post-selection. Dot-dashed line: calculated theoretical prediction of the experiment.

We also characterized the experiment in terms of the purity of the post-selected output state, defined as $\mathcal{P} = \text{tr}(\rho_{\text{out}}^2)$. In the case of Gaussian states, the purity of the output state can be expressed as $\mathcal{P} = (V_{\text{out}}^+ V_{\text{out}}^-)^{-1/2}$. In the ideal case of a lossless experiment and a post-selection threshold $X_{\text{r}}^+ = 0$, the protocol is a purity preserving transform, independent of the input state and the amount of squeezing of the ancilla state. In the experiment, as the input states are slightly mixed, we calculate the purity of the post-selected output state, normalized to the purity of the input state, which is given by $\mathcal{P}_{\text{norm}} = (V_{\text{out}}^+ V_{\text{out}}^-)^{-1/2} / (V_{\text{in}}^+ V_{\text{in}}^-)^{-1/2}$. Fig. 5 (b) shows the experimental purity of the post-selected output state for varying input states, which illustrates how the purity is improved

via the post-selection process. For a beam splitter reflectivity of $R = 0.75$ we achieved a best purity of $\mathcal{P}_{\text{norm}} = 0.81 \pm 0.04$ for an input state of $|\gamma^+| = 2.03 \pm 0.02$. Fig. 5 (b) shows that the purity of the post-selected output states were approximately independent of the input states, for a large range of input states.

We also implemented our scheme for a beam splitter reflectivity of $R = 0.5$. In this case, we measured a best fidelity of $\mathcal{F}_{\text{ave}} = 0.96 \pm 0.01$, which exceeded the maximum classical fidelity of $\mathcal{F}_{\text{clas}} = \sqrt{8}/3 \approx 0.94$, and measured a best purity of $\mathcal{P}_{\text{norm}} = 0.80 \pm 0.04$.

In summary, we have investigated a continuous-variable conditioning scheme based on a beam splitter interaction, homodyne detection and an ancilla squeezed vacuum state. The conditional evolution of quantum systems based on continuous-variable measurements of the ancilla state are of particular interest as they can yield from input Fock states, non-Gaussian states, which have applications in the field of quantum information. Further, for Gaussian states, this technique provides an alternative to continuous electro-optic feed-forward schemes. We theoretically showed that our conditional post-selection scheme yields high fidelity squeezed single photon and superposition of coherent states from input one and two photon Fock states respectively, for realizable squeezing of the ancilla state. We experimentally demonstrated the principles of this scheme using coherent states, and measured experimental fidelities that were only achievable using quantum resources.

We thank the Australian Research Council for financial support through the Discovery Program.

-
- [1] M. Nielsen and I. Chuang, *Quantum computation and quantum information* (Cambridge University Press, Cambridge, UK 2000).
 - [2] J. L. O'Brien *et al.*, *Nature* **426**, 264 (2003).
 - [3] E. Knill, R. Laflamme, G. J. Milburn, *Nature* **409**, **46** (2001).
 - [4] M. Dakna, J. Clausen, L. Knöll, D.-G. Welsch, *Phys. Rev. A* **59**, 1658 (1999); J. Clausen, M. Dakna, L. Knöll, D.-G. Welsch, *Opt. Commun.* **179**, 189 (2000).
 - [5] J. Laurat *et al.*, *Phys. Rev. Lett.* **91**, 213601 (2003).
 - [6] S. A. Babichev, B. Brezger, A. I. Lvovsky, *Phys. Rev. Lett.* **92**, 047903 (2004).
 - [7] T. C. Ralph, A. P. Lund, H. M. Wiseman, *J. Opt. B: Quantum Semiclass. Opt.* **7** S245S249 (2005).
 - [8] H. Jeong, M. S. Kim, J. Lee, *Phys. Rev. A* **64**, 052308 (2001); T. C. Ralph *et al.*, *Phys. Rev. A* **68**, 042319 (2003).
 - [9] A. P. Lund, H. Jeong, T. C. Ralph, M. S. Kim, *Phys. Rev. A* **70**, 020101(R) (2004).
 - [10] R. Filip, P. Marek, U. L. Andersen, *Phys. Rev. A* **71**, 042308 (2005); P. K. Lam, T. C. Ralph, E. H. Huntington, H.-A. Bachor, *Phys. Rev. Lett.* **79**, 1471 (1997).
 - [11] W. P. Bowen *et al.*, *Phys. Rev. A* **67**, 032302 (2003); A. M. Lance *et al.*, *Phys. Rev. Lett.* **92**, 177903 (2004).